Earth's Future

RESEARCH ARTICLE
10.1029/2022EF003427

Emergent Constraint for Future Decline in Arctic Phytoplankton Concentration

Kyung Min Noh[1], Hyung-Gyu Lim[2,3], Eun Jin Yang[4], and Jong-Seong Kug[1,5]

[1]Division of Environmental Science and Engineering, Pohang University of Science and Technology (POSTECH), Pohang, South Korea, [2]Princeton University/Atmospheric and Oceanic Sciences Program, Princeton, NJ, USA, [3]Scripps Institution of Oceanography, University of California San Diego, La Jolla, CA, USA, [4]Division of Ocean Sciences, Korea Polar Research Institute, Incheon, South Korea, [5]Institute for Convergence Research and Education in Advanced Technology, Yonsei University, Seoul, South Korea

Abstract In recent decades, the Arctic Ocean has experienced continuous warming and freshening, affecting biogeochemical factors such as nutrient supply, light availability, chlorophyll, and productivity. While Arctic marine productivity is projected to increase due to the expansion of the open ocean and increased chlorophyll concentration, uncertainties related to chlorophyll and nutrients may distract the fidelity of productivity in current Earth system models (ESMs). Here, we analyze the existing uncertainty in the Arctic chlorophyll projections using the 26 ESMs participating in Coupled Model Intercomparison Projects 5 and 6 (CMIP5 and CMIP6). We found that the uncertainty in the Arctic chlorophyll projections in the CMIP6 ESMs is greater than in the CMIP5 ESMs due to increasing uncertainty in the background nitrate concentration. A significant relationship between background nitrate and projected chlorophyll ($r = 0.86$) is demonstrated using the observational climatology of nitrate. Based on this strong relationship, the emergent constraint is applied to reduce the uncertainty of future chlorophyll projections. Declines in chlorophyll concentration based on emergent constraint are estimated to be further decreased in the future ($44.9\% \pm 29.1\%$ to $50.9\% \pm 27.6\%$) than at present, which is about three-fold larger than the multi-model mean projection ($-13.5\% \pm 48.7\%$). Comparing cumulative density functions before and after the emergent constraint, the probability of the decreasing chance of chlorophyll is increased by approximately 36% from 60% in prior CMIP5,6 to 93%–96% after constraint. Our results imply that reducing the uncertainty in background nitrate concentration can improve the fidelity of future projections of the Arctic ecosystem in the ESMs.

Plain Language Summary The Arctic Ocean environment has undergone changes in response to human-induced greenhouse gases, such as dramatic warming and sea-ice retreat. Recently, the chlorophyll concentration, the proxy of the phytoplankton biomass, has increased leading to an increase in marine productivity in the Arctic Ocean. However, there is a large uncertainty in the current earth system models (ESMs) regarding future changes in phytoplankton biomass. In this study, we analyze the 26 ESMs and estimate the future changes in phytoplankton biomass based on the relationship between current climate and future changes, which is known as the "emergent constraint." We find a strong relationship between the level of current nitrate levels and future chlorophyll changes in the Arctic Ocean. Based on this relationship, we estimate the uncertainty of the Arctic chlorophyll decline, which is about three times larger than the multi-model mean projection. Our results suggest that reducing the uncertainty of present-climate nitrate in the ESMs is important for projecting Arctic productivity.

Key Points:

- The CMIP6 models exhibit twice the inter-model diversity in chlorophyll concentration compared to the CMIP5 models in the Arctic Ocean
- The large uncertainty in the Arctic chlorophyll projections is caused by the magnitude of the simulated summer nitrate climatology
- Constrained by the nitrate observations, the future decline in Arctic chlorophyll is estimated to be three times larger than the multi-model mean

Supporting Information:

Supporting Information may be found in the online version of this article.

Correspondence to:

H.-G. Lim and J.-S. Kug,
hyl021@ucsd.edu;
jskug1@gmail.com

Citation:

Noh, K. M., Lim, H.-G., Yang, E. J., & Kug, J.-S. (2023). Emergent constraint for future decline in Arctic phytoplankton concentration. *Earth's Future*, *11*, e2022EF003427. https://doi.org/10.1029/2022EF003427

Received 14 DEC 2022
Accepted 20 MAR 2023

Author Contributions:

Conceptualization: Kyung Min Noh, Hyung-Gyu Lim, Jong-Seong Kug
Data curation: Kyung Min Noh
Formal analysis: Kyung Min Noh, Hyung-Gyu Lim
Funding acquisition: Hyung-Gyu Lim, Jong-Seong Kug
Investigation: Kyung Min Noh, Hyung-Gyu Lim
Methodology: Kyung Min Noh, Hyung-Gyu Lim, Eun Jin Yang, Jong-Seong Kug

1. Introduction

The global climate has been affected by rising greenhouse gas concentrations, which are driving a rapid warming of the Arctic region (Hartmann et al., 2013). And the warming rate in the Arctic is expected to experience more than twice the global average warming (AMAP, 2017). Arctic warming has led to physical manifestations such as increased sea ice melt (AMAP, 2017; Ardyna & Arrigo, 2020; Kwok, 2018), enhanced vertical stability (Polyakov et al., 2018; Toole et al., 2010), increased river runoff (Ahmed et al., 2020; Lammers et al., 2001; Peterson et al., 2002), and strengthened upper ocean currents (Polyakov et al., 2020; Timmermans & Marshall, 2020). These environmental changes have also affected the phytoplankton dynamics by decreasing nutrient supplies (Tremblay et al., 2015) and increasing the amount of light transmitted through the water column (Jönsson et al., 2020). Recent studies have reported that these environmental changes have affected the phytoplankton

Project Administration: Hyung-Gyu Lim, Eun Jin Yang, Jong-Seong Kug
Resources: Eun Jin Yang, Jong-Seong Kug
Software: Kyung Min Noh
Supervision: Hyung-Gyu Lim, Jong-Seong Kug
Visualization: Kyung Min Noh
Writing – original draft: Kyung Min Noh
Writing – review & editing: Kyung Min Noh, Hyung-Gyu Lim, Eun Jin Yang, Jong-Seong Kug

phenology, including the phytoplankton community and size (Fujiwara et al., 2016; Lee et al., 2019; Neeley et al., 2018), the timing of phytoplankton blooms (Kahru et al., 2011; Tremblay et al., 2006; Yamaguchi et al., 2022), and phytoplankton biomass (Lewis et al., 2020). These changing Arctic phytoplankton dynamics have altered the marine Arctic ecosystems shifting species distributions and altering trophic levels (Ardyna & Arrigo, 2020).

According to satellite observations, marine productivity in the Arctic Ocean has increased by 57% over the past 20 years (Arrigo & van Dijken, 2011, 2015; Lewis et al., 2020). Sea ice retreat and an increase in the number of blue ocean days enhance the light availability over the Arctic Ocean and thus the increase in net primary production (NPP). However, an increase in chlorophyll concentration has been a major contributor to the increase in NPP over the past decades, due to the increased nutrient supply from subsurface waters rather than sea-ice retreat (Lewis et al., 2020). Similarly, the current generation of Earth system models (ESMs) simulated increased NPP in the Arctic Ocean in response to greenhouse gas emission scenarios (Bopp et al., 2013; Kwiatkowski et al., 2020). Although nearly all ESMs simulated the same direction of NPP changes, the intensity of increased NPP in the Arctic Ocean still shows large uncertainty (Tagliabue et al., 2021). Since Arctic phytoplankton growth is dominated by the nitrate availability and sea-ice concentrations (Long et al., 2021; Simpson et al., 2008; Stock et al., 2020; Tremblay et al., 2015; Tremblay & Gagnon, 2009), the extent of nitrate depletion in the upper ocean plays an important role in determining the future NPP changes (Vancoppenolle et al., 2013).

Depth-integrated NPP is typically estimated as a product of phytoplankton carbon or biomass and an empirical formula describing its physiological dependence on temperature, light, and nutrients (Behrenfeld et al., 2005; Behrenfeld & Falkowski, 1997). All ESMs show the decreases in sea ice and the resulting increase in light availability over the Arctic Ocean (Davy & Outten, 2021; Notz & SIMIP Community, 2020). Therefore, the importance of the estimating chlorophyll concentration, usually considered a proxy for the phytoplankton biomass, has received more attention to quantify future changes in Arctic marine productivity (Lewis et al., 2020). In addition, phytoplankton play an important role in the physics of the upper ocean by modifying the light penetration, leading to bio-optical feedbacks (Manizza et al., 2005). Enhanced attenuation of shortwaves by changes in the Arctic chlorophyll may amplify Arctic warming (Lengaigne et al., 2009; Lim et al., 2019a, 2019b; Park et al., 2015). Therefore, the fidelity of a future projection of chlorophyll concentration is essential for estimating changes in the Arctic climate and marine ecosystem resilience.

However, strong uncertainties in simulated chlorophyll concentrations exist and have not improved or even worsened in CMIP6 compared to CMIP5 (Séférian et al., 2020). To reduce this uncertainty in future chlorophyll changes, we applied the emergent constraint method, which is a useful approach based on the relationship between the current climate state and future climate changes (Hall et al., 2019). Emergent constraints have been widely applied to various components of the Earth system such as climate sensitivity (Brient et al., 2016; Zhai et al., 2015), the hydrological cycle (Li et al., 2017; O'Gorman, 2012), and the Arctic climate change (Boe et al., 2009; Bracegirdle & Stephenson, 2013). In particular, the future projections in marine biogeochemistry have been estimated by emergent constraints, such as, the primary production in tropical oceans (Kwiatkowski et al., 2017), the acidification in the Arctic Ocean (Terhaar et al., 2020), and the anthropogenic carbon sink in the Southern Ocean (Terhaar, Frölicher, & Joos, 2021). Despite various studies on Arctic phytoplankton, realistic estimations in Arctic chlorophyll changes have not been performed based on the relationship between the present climate and ESM simulated projections.

Here, we analyzed the future changes in Arctic chlorophyll concentration under different climate change scenarios and suggested the importance of current level of nitrate concentration using ESM archives participating in CMIP5 and CMIP6. We applied the emergent constraint method (Hall et al., 2019) by considering nitrate uncertainties with observed values and their intermodal diversities to estimate the corrected future Arctic chlorophyll changes. Detailed descriptions of the ESMs and methods are provided in Section 2. Results of the high uncertainties in Arctic nitrate and chlorophyll and future chlorophyll estimation based on the emergent constraint are presented in Section 3. A summary and discussion of the implications of the present results are given in Section 4.

2. Data and Methods

We employ the two different generations of ESM outputs simulated by the CMIP5 (Taylor et al., 2012) and CMIP6 ESMs (Eyring et al., 2016). Twenty-six ESMs with embedded marine biogeochemical models have prognostically

simulated nitrate and chlorophyll concentrations interacting with the climate system. Further information on the individual models and institutions used in this study is provided in Tables S1 and S2 in Supporting Information S1, respectively. We use historical simulations covering the periods 1900–2005 (CMIP5) and 1900–2014 (CMIP6). And different the Intergovernmental Panel on Climate Change scenarios, covering the periods up to the end of the twenty-first century, are compared with the present Arctic climate. The scenarios are called Representative Concentration Pathways (RCPs) in CMIP5 (Moss et al., 2010) and Shared Socio-economic Pathways (SSPs) in CMIP6 (O'Neill et al., 2016). To estimate the responses to future pathways of greenhouse gas emissions, we use three different emission scenarios, namely, SSP1-2.6, SSP2-4.5, and SSP5-8.5, and compare the results. In the business-as-usual scenario (SSP5-8.5), the peak of radiative forcing is not reached until the end of the twenty-first century. Corresponding to the SSP scenarios, RCP 2.6, RCP4.5, and RCP8.5 are used in CMIP5.

Model outputs are re-gridded using distance-weighted average remapping (climate data operators; remapdis) to the one-degree horizontal resolutions for the intercomparison within ESMs (Schulzweida, 2019). Chlorophyll and nitrate concentrations are averaged for the Arctic Circle, latitudes above 66.5°N (Arrigo & van Dijken, 2011). The changes in chlorophyll and nitrate are defined as the difference in the variables between the period 1981–2000 and the period 2080–2099. To calculate the rate of change of the chlorophyll concentration, the changes are normalized by dividing the difference by the Arctic mean value for the period 1981–2000.

Two different nitrate concentration datasets based on in situ reanalysis, the World Ocean Atlas 18 (WOA18) (Garcia et al., 2018) and the Global Ocean Data Analysis Project version 2 (GLODAPv2) (Lauvset et al., 2016) datasets, are used to apply the emergent constraint method. Both WOA18 and GLODAPv2 datasets provide present-day values in the Arctic nitrate climatology interpolated to $1° \times 1°$ latitude–longitude grids. And their total uncertainty is derived from the standard deviations of nitrate concentration for each grid cell and each month in both WOA18 and GLODAPv2 datasets. We defined the background nitrate concentration as the current climate level of nitrate concentration, which is averaged over the last 20 years of the twentieth century (historical scenario). Background nitrate from reanalysis datasets is used as a standard level of baseline nitrate concentration to check model fidelity and to estimate corrected values in chlorophyll projections using the emergent constraint based on the relationship between background nitrate and chlorophyll changes in CMIP5 and CMIP6.

The emergent constraints are based on strong statistical relationships between current states and future projections. Constraining the diverse future chlorophyll changes with present-day nitrate observations can reduce the uncertainty of their projections. Least-squares linear regressions are calculated from the simulated chlorophyll changes and background nitrate. And the probability density functions (PDFs) of the chlorophyll projections are calculated following the previously established framework (Cox et al., 2013; Kwiatkowski et al., 2017). The constrained PDFs of the Arctic chlorophyll changes are calculated with the unconstrained (prior) CMIP5 and CMIP6 ESM projections and present-climate in-situ based observations (GLODAPv2 and WOA18). The prior PDF is assumed to be uniformly distributed across ESM ensembles and follows a Gaussian distribution. To avoid an extreme model dependence on emergent relationships (Hall et al., 2019), we perform the emergent constraint after excluding single model in total 26 CMIP5 and CMIP6 models and average these constrained estimations (hereafter out-of-sample testing).

3. Results

3.1. Higher Uncertainty in CMIP6 Chlorophyll Projections

The multi-model ensemble (MME) in chlorophyll concentration in the Arctic Ocean is projected to decrease by 30%, with a range of 7%–55%, under the RCP85 scenario in CMIP5 (Figure 1a). In higher emission scenarios, chlorophyll and nitrate concentrations are projected to decrease greater (Table S3 in Supporting Information S1). The nitrate decrease may explain the chlorophyll decrease (Figure 1b), which is projected to decrease by 46%—with a range of 25%–66%—due to the enhanced stratification resulting from upper ocean warming and freshening (Figure S1 in Supporting Information S1). The ensemble mean of CMIP6 models projects a small increase in chlorophyll (an average of 4.1% for the SSP5-85 scenario), but there is a remarkably wide range of projections from a decrease of 56% to an increase of 64% (Figure 1c). Some models project an increase in chlorophyll despite the projected decrease in nitrate concentration in the Arctic Ocean of 49%—ranging from 31% to 68%—for the CMIP6 models (Figure 1d). The other models also show decreases in both the chlorophyll and nitrate in response to the increased radiative forcing (Figures S2 and S3 in Supporting Information S1). Possibly due to the

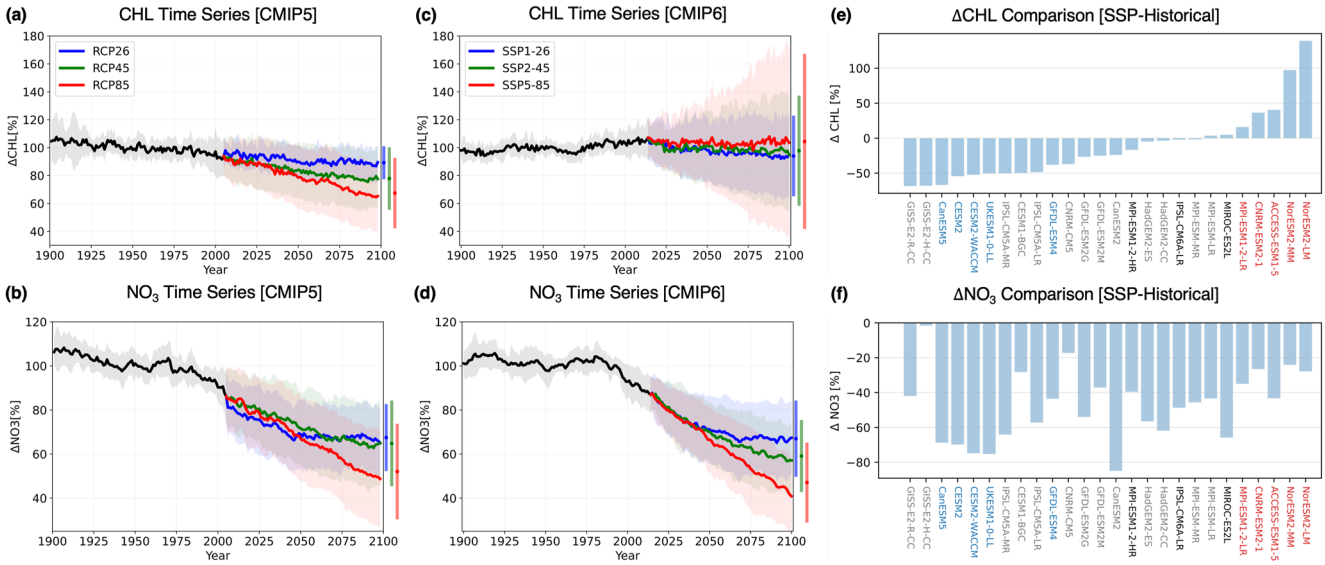

Figure 1. Projections of chlorophyll and nitrate concentration in the Arctic Ocean. Time series of the annual mean chlorophyll (a and c) and nitrate (b and d) concentrations projected by Coupled Model Intercomparison Projects 5 and 6 (CMIP5 and CMIP6) models were averaged for the Arctic Ocean (the region above 66.5°N) and normalized using the average values for the Arctic region obtained from historical data for 1981–2000. Colors indicate different scenarios: historical (black), RCP26 and SSP1-26 (blue), RCP45 and SSP2-45 (green), and RCP85 and SSP5-85 (red). Shadings indicate a range of ± 1 inter-model standard deviations in chlorophyll and nitrate changes for each scenario, and the thick lines represent the ensemble means for CMIP models. Bar graphs illustrate a range of ±1 inter-model standard deviations of changes averaged in the last 20 years (2080–2099) with multi-model ensemble (MME) (scatter). Time series of the chlorophyll and nitrate projections for the individual model are provided (Figures S2 and S3 in Supporting Information S1). (e) Projected changes in chlorophyll concentration under RCP85 and SSP5-85 (for the period 2080–2099 relative to historical simulations for 1981–2000) averaged over the Arctic Ocean area (>66.5°N) are arranged according to the size of the projected change in chlorophyll concentration. (f) Projected changes in nitrate concentration relative to historical simulations (for 1981–2000) arranged by the model in the same order as in (e). The model names are colored according to the group they belong to CMIP5 (gray), CMIP6-negative (blue), CMIP6-positive (red), and remained CMIP6 (black).

wide range of chlorophyll projections, the amplitudes of the MME in chlorophyll changes get smaller in response to the stronger radiative forcing scenario become smaller from a decrease of 4% (SSP1-2.6) to an increase of 4% (SSP5-8.5) in CMIP6 (Table S3 in Supporting Information S1). The results are consistent with previous studies suggesting that CMIP6 models have not only a greater climate sensitivity (Zelinka et al., 2020) but also a higher uncertainty in future chlorophyll concentrations than CMIP5 models (Kwiatkowski et al., 2020).

The projected changes in the chlorophyll concentration for the business-as-usual scenario with the greatest radiative forcing (RCP85 and SSP5-85) are arranged in the order of chlorophyll changes (Figure 1e). Seven CMIP6 models project an increase in the chlorophyll concentration, while the remaining CMIP5 and CMIP6 models project a decrease. To understand the cause of the inter-model diversity within the ESM projections in chlorophyll, we also examined the corresponding projected changes in the nitrate concentration and arranged the results in the same order as the chlorophyll changes (Figure 1f). Although nitrate availability is a critical component driving differences in the Arctic ecosystem simulations (Cabré et al., 2014; Vancoppenolle et al., 2013), the relationship between the changes in the nitrate and the chlorophyll concentration is not clear ($r = 0.31$) as shown in Figures 1e and 1f. This weak relationship implies that the large inter-model diversity in chlorophyll projections cannot be fully explained by projected changes in nitrate concentration. To understand the inter-model diversity in projected chlorophyll concentration, a detailed analysis of the seasonality and mean state of nitrate concentration is required.

3.2. Emergent Relationship Between Arctic Chlorophyll Changes and Background Nitrate

To identify the main reason for the inter-model diversity in chlorophyll changes, we classified the CMIP models into three groups—CMIP5, CMIP6-negative, and CMIP6-positive—based on the projected changes in the chlorophyll concentration (see Figures 2a–2c). To compare the different CMIP6 groups, the five most increased and decreased models are classified into CMIP6-negative and CMIP6-positive groups. In general, CMIP5 and CMIP6-negative models show a decrease in the chlorophyll concentration. In contrast, although

10.1029/2022EF003427

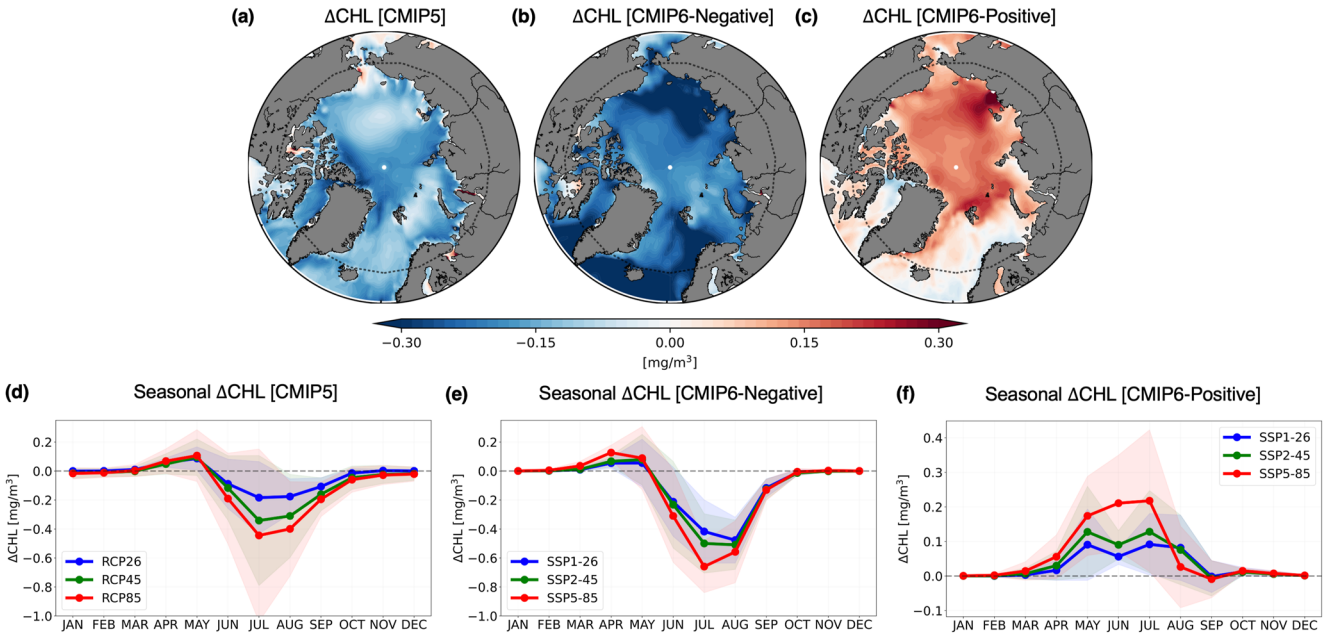

Figure 2. Projections of the spatial distribution and seasonal changes in chlorophyll concentration. (a–c) The composite maps show the projected changes in annual mean chlorophyll concentration for the period 2080–2099 compared to 1981–2000 under RCP85 and SSP5-85 for the different groups of models: (a) CMIP5, (b) CMIP6-negative, and (c) CMIP6-positive. The dotted lines represent the Arctic Circle (>66.5°N). Contours maps of the chlorophyll concentration changes for the individual model are provided in Figure S5 in Supporting Information S1. (d–f) The seasonal changes in chlorophyll concentration are shown for the (d) CMIP5, (e) CMIP6-negative, and (f) CMIP6-positive models. The different colors indicate different scenarios: RCP26 and SSP1-26 (blue), RCP45 and SSP2-45 (green), and RCP85 and SSP5-85 (red). Shadings indicate a range of ± 1 inter-model standard deviations in chlorophyll changes for different scenarios, and the thick lines represent the ensemble means for three groups and three scenarios.

the increase in the North Atlantic Ocean and the Barents Sea is relatively small, CMIP6-positive models show increases in chlorophyll over almost the whole Arctic Ocean. The results suggest that the differences between the model chlorophyll projections are not limited to the specific region but occur in almost the entire Arctic Ocean.

Due to the strong seasonal variability of the sea ice, surface temperature, and stratification in the Arctic Ocean (Wassmann & Reigstad, 2011), we further analyzed the seasonality in the projected chlorophyll changes for three groups and the different emission scenarios (Figures 2d–2f). All groups project the same increases in chlorophyll during the boreal spring (March to May; MAM). However, the chlorophyll changes in the boreal summer are simulated very differently (June to August; JJA). The increased chlorophyll in the boreal spring is related to the limited amount of light due to sea ice cover. The more pronounced bloom in the spring is projected in response to the higher emission scenarios (i.e., SSP5-85 and RCP85) than the lower emission scenarios (i.e., SSP1-26, RCP26). As the sea-ice melts more and earlier in response to greenhouse warming, the light may become more available with abundant nutrients that have accumulated over the winter (December to February; DJF). In the nutrient-rich environment, the increased light leads to an earlier bloom of the phytoplankton and the increase in the amount of chlorophyll (Assmy et al., 2017; Kahru et al., 2011; Park et al., 2015; Tremblay et al., 2006). However, in the boreal summer, two factors—light and nutrients—are affected by warming in opposite ways. On the one hand, the amount of available light may increase in response to the decrease in sea ice, which tends to increase the chlorophyll concentration. On the other hand, the enhanced static stability contributes to nutrient reduction (Kwiatkowski et al., 2020) due to the increased surface warming, and the ocean freshening caused by the sea ice melting (see Figure S4 in Supporting Information S1). The enhanced nutrient limitation leads to the reduction in chlorophyll concentration. Therefore, in the presence of two opposing limiting factors, the chlorophyll response will be determined by the relative strength of the two limiting factors.

To show the different patterns of seasonality in the three groups, we compared the changes in chlorophyll concentration between the business-as-usual scenario and the historical scenario, as well as mean states in nutrient limitation in the historical scenario in the three groups (Figure 3). To estimate the nitrate limitation in different

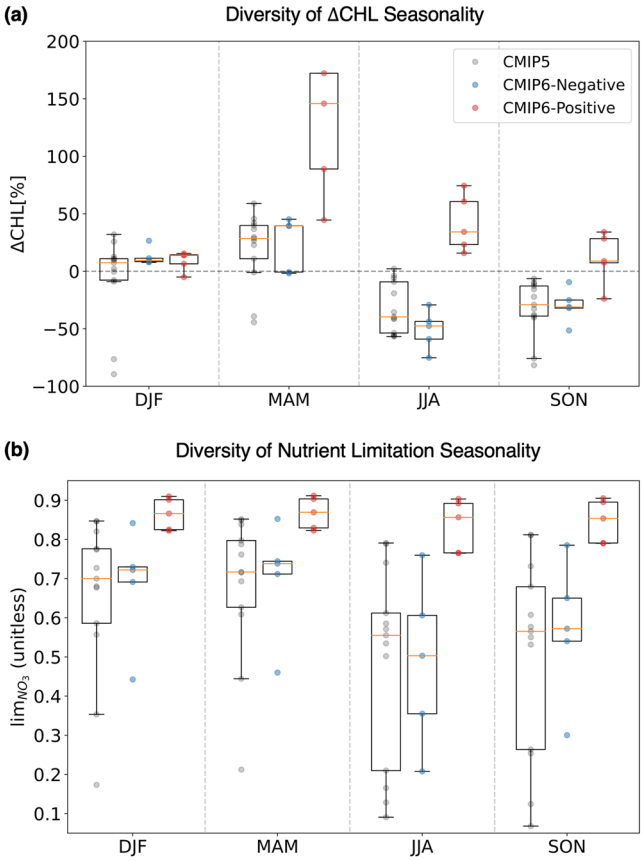

Figure 3. Range of seasonality in (a) chlorophyll changes and (b) nutrient limitations. The boxes denote the interquartile range between the 25th and 75th percentiles, and the median value for each group is marked by a horizontal orange line. The value projected by the individual model is plotted as a colored dot according to the group to which the model belongs: CMIP5 (gray), CMIP6-negative (blue), and CMIP6-positive (red). Detailed information on the seasonal changes in the chlorophyll concentration and nutrient limitation of the individual model are provided in Figure S6 in Supporting Information S1.

model parameterizations (Laufkotter et al., 2015), we defined the general nitrate limitation (lim_{NO_3}) as the half-saturation coefficient (Michaelis & Menten, 1913) used in Vancoppenolle et al. (2013):

$$\mathrm{lim}_{NO_3} = \frac{NO_3}{K_{NO_3} + NO_3}$$

where $K_{NO_3} = 1.6\ \mathrm{mmol/m^3}$ is the half-saturation concentration for the nitrate uptake as the value of the nitrate uptake by diatoms (Sarthou et al., 2005). The value of the nutrient limitation is determined by Liebig's law of the minimum of different nutrient limitations, such as nitrate, phosphate, silicate, and trace metals. As the Arctic Ocean is typically nitrate-depleted (Tremblay et al., 2015; Yamamoto-Kawai et al., 2006), the dominant limiting nutrient for phytoplankton growth is known as nitrate in the following analysis (Long et al., 2021; Stock et al., 2020; Vancoppenolle et al., 2013).

In the boreal winter and spring seasons, the enhanced light availability resulting from a reduction in sea ice (Figure S4 in Supporting Information S1) leads to an increase in chlorophyll concentration in the projections simulated by most CMIP5 and CMIP 6 models (DJF and MAM columns in Figure 3a). Note that the CMIP6-positive models project a larger increase in chlorophyll, implying that the CMIP6-positive models are more sensitive to light availability. In summer, the CMIP5 and CMIP6-negative models project a decrease in chlorophyll, while the CMIP6-positive models project an increase. The different seasonality in the chlorophyll projections results from the different seasonality of nutrient limitation in the three groups. In winter and spring, nutrients are relatively abundant, which is consistent with the weak nutrient limitation (DJF and MAM columns in Figure 3b) resulting from deep convection in the cold seasons. In the weak nitrate limitation, the additional light availability may provide a favorable environment for the growth of phytoplankton.

However, in the boreal summer, the nutrient decrease is caused by the increased uptake by phytoplankton in spring and the reduced entrainment from deep water, which leads to more severe nutrient limitation (JJA column in Figure 3b). In contrast, the CMIP6-positive models, however, show a similar weak nutrient limitation in summer as in winter and spring. The CMIP6-positive models also project a decrease in nitrate concentration like the other groups, but the amount of nitrate is still large enough to supply nitrate to phytoplankton. And the contrast of nutrient limitation between the CMIP6-positive models and the others becomes larger in a warming climate (Figure S7 in Supporting Information S1). Although all ESMs project an increase in light availability due to the sea ice melting, the CMIP5 and CMIP6 ESMs project a large spread in the future chlorophyll changes due to the different seasonality of nutrient limitation in the Arctic Ocean.

3.3. Emergent Constraints on Phytoplankton Biomass in Earth System Models

In contrast to the weak relationship between future chlorophyll changes and the changes in sea surface temperature, sea ice, and nitrate concentrations (Figure S10a in Supporting Information S1), the clear difference in the background nitrate concentration among the three groups (Figure S8 in Supporting Information S1) suggests that the background nitrate is critical for determining future changes in the chlorophyll concentration in the Arctic. To further illustrate the importance of background nitrate more clearly, the relationship between the background nitrate concentration and the change in chlorophyll concentration is shown for three different emission scenarios (Figures 4a–4c). In the high emissions scenario, the relationship between the background nitrate concentration and the projected change in chlorophyll exhibits a strikingly high positive correlation ($r = 0.86$, $P < 0.001$) in the total 26 CMIP5 and CMIP6 ESMs, which is also significant across other scenarios such as SSP1-2.6 ($r = 0.66$) and SSP2-4.5 ($r = 0.80$).

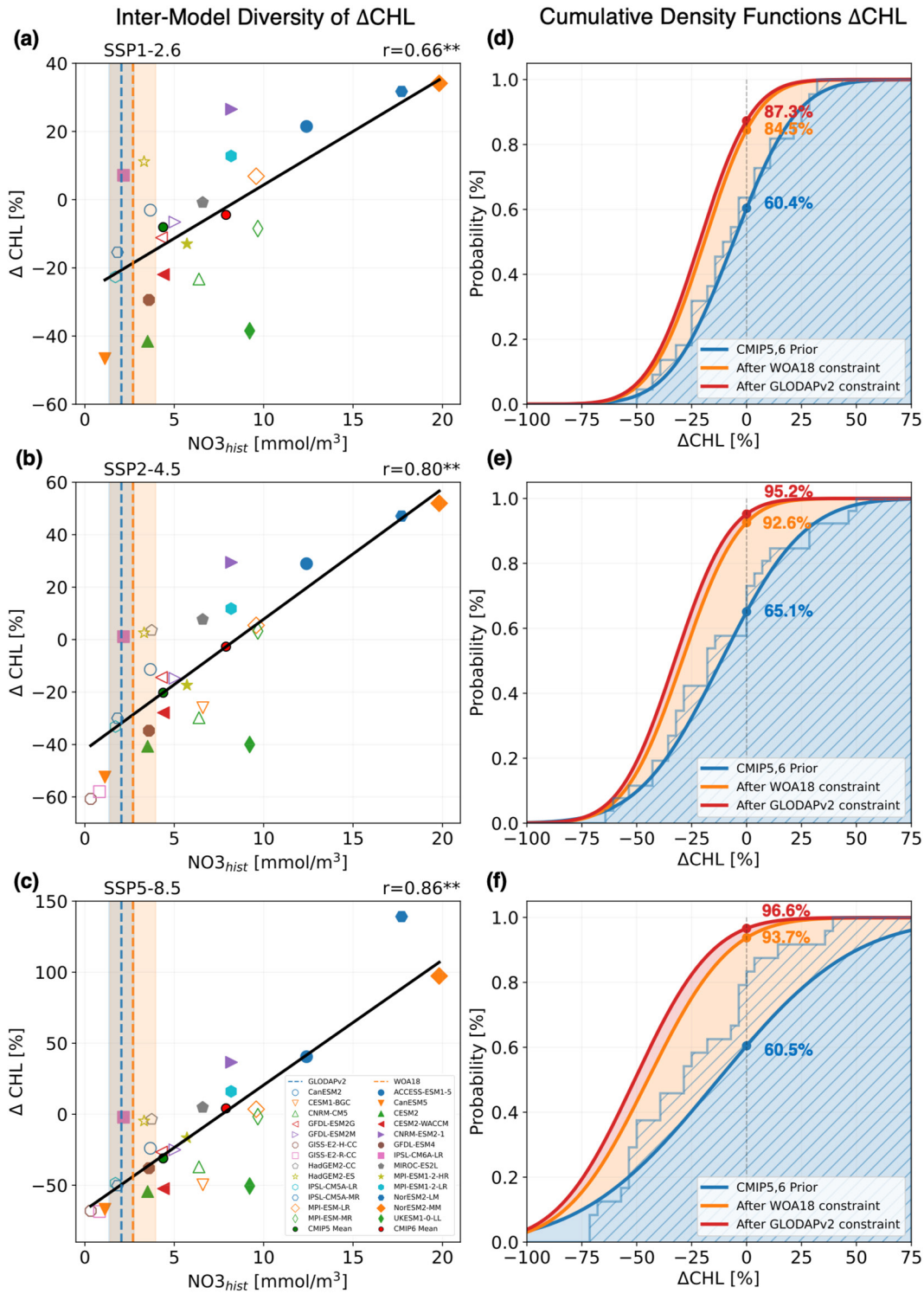

Figure 4.

The CMIP6 models have diverse background nitrate concentrations, and the inter-model diversity leads to greater uncertainty in the chlorophyll projections than in the CMIP5 models. In CMIP6-positive models, although the enhanced stratification decreases the nitrate by 3.8 mmol/m^3, the background nitrate is still too high to limit the phytoplankton growth. Under the weak nitrate limitation in CMIP6-positive models, the chlorophyll concentration increases in response to the weakened light limitation. However, the same weakened light limitation does

Table 1
The Arctic Mean Changes in Chlorophyll Obtained for Different Scenarios Before and After Emergent Constraint

Scenario	CMIP5,6 prior [%]	After WOA18 constraint [%]	After GLODAPv2 constraint [%]
SSP1-2.6	−5.9 (± 22.7)	−19.1 (± 18.8)	−21.3 (± 18.6)
SSP2-4.5	−11.5 (± 29.7)	−29.2 (± 20.2)	−32.7 (± 19.5)
SSP5-8.5	−13.5 (± 48.7)	−44.9 (± 29.1)	−50.9 (± 27.6)

Note. The error ranges given are the standard deviation of chlorophyll projections, and standard errors of probability density functions, which are constrained by WOA18 and GLDOAPv2 background nitrate concentration, respectively. Out-of-sample testing is applied across different ESM ensembles.

not lead to an increase in chlorophyll concentration in CMIP6-negative and CMIP5 models because the nitrate is depleted in the chlorophyll decreasing groups. While the Arctic background nitrate in the reanalysis ranges from about 2.0 mmol/m^3 (from GLODAPv2) to 2.7 mmol/m^3 (from WOA18), the simulated Arctic background nitrate in the CMIP5 and CMIP6 models is about 6.1 mmol/m^3 with a range from 0.3 to 19.8 mmol/m^3. This indicates that current models tend to overestimate the background nitrate concentration. In particular, the CMIP6-positive models have a strong positive bias (10.6–11.2 mmol/m^3) in the background nitrate concentration, which may contribute to projecting excessive increases in the chlorophyll concentration.

Despite the systematic biases in background nitrate in the ESMs, the high correlation between the background nitrate concentration and future changes in the chlorophyll concentration provides an opportunity to make credible projections of Arctic chlorophyll. Applying the emergent constraints based on the linear relationship between the projected changes in the chlorophyll concentration and the background nitrate concentrations used in climate models, the estimated chlorophyll concentration is decreased by 44.9 ± 29.1% (based on WOA18) to 50.9 ± 27.6% (based on GLODAPv2) compared to the current level in response to the business-as-usual scenario. The observation-based estimation is larger than the decrease in projection corresponding to MME (13.5 ± 48.7%) under CMIP5 and CMIP6 ESMs, and the more decreased estimations in MME in other scenarios support the robustness of the emergent constraint (Table 1). In addition, we applied the out-of-sample testing in both CMIP5 and CMIP6 respectively, which exhibits similar ranges of chlorophyll changes (Table S4 in Supporting Information S1). This result suggests that current ESMs tend to underestimate the reduction in Arctic chlorophyll due to overestimated background nutrients.

Cumulative density functions (CDF) in chlorophyll changes from before and after the constraints are compared across scenarios (Figures 4d–4f). The CDFs provide information about the reduced uncertainty in the direction of the chlorophyll projections. Before the emergent constraint, the probability of the decreased chlorophyll projections in business-as-usual scenarios is about 60%, which implies that there is still a 40% possibility of the increased chlorophyll projections (Figure 4f). After the emergent constraint, the probability of the decreased chlorophyll increases to 93%–96%. In other words, the uncertainty of the estimated chlorophyll changes is reduced by about 33% (based on WOA18) to 36% (based on GLODAPv2). The reduced uncertainties are similar for the other scenarios (Figures 4d and 4e). Therefore, we can strongly suggest that chlorophyll is projected to decrease under the current level of background nitrate concentration with more than 90% probability.

Future changes in NPP are strongly associated with future changes in chlorophyll with a high correlation ($r = 0.85$, $P < 0.001$) (Figure S10b in Supporting Information S1) because chlorophyll can affect photosynthetic rates (Behrenfeld & Falkowski, 1997). Although the parameterization of NPP in the ESMs differs, NPP was generally calculated by vertical integration of the product between phytoplankton biomass and its growth rate in phytoplankton species. The link between chlorophyll and NPP implies the importance of simulating the fidelity in background nitrate concentration for estimating the future changes in Arctic marine productivity, as the nitrate fluxes are important to Arctic primary production (Randelhoff et al., 2020). The NPP changes are a matter of chlorophyll rather than other physical environments such as sea ice and surface temperature in CMIP5

Figure 4. Constrained projections of chlorophyll concentration. (a–c) Scatter plots showing the changes in chlorophyll concentration compared to historical simulations plotted against the background nitrate concentration under different scenarios: RCP26 and SSP1-26 (a), RCP45 and SSP2-45 (b), and RCP85 and SSP5-85 (c). The annual mean values of the background nitrate concentration and the change in chlorophyll concentration averaged over the Arctic Ocean are plotted for individual model; the open and filled markers represent Coupled Model Intercomparison Project 5 (CMIP5) models and CMIP6 models, respectively. The thick black solid line is the linear regression line between the background nitrate concentration and the change in chlorophyll concentration for all CMIP5 and CMIP6 models. The vertical blue and orange dashed lines mark the average background nitrate concentration in the Arctic Ocean according to the GLODAPv2 and WOA18 observations with associated uncertainty (shaded area). Constrained estimation using standard error is given in Table S5 in Supporting Information S1. (d–f) Cumulative density functions (CDFs) of chlorophyll changes in CMIP5 and CMIP6, and constrained changes based on observations under different scenarios: RCP26 and SSP1-26 (d), RCP45 and SSP2-45 (e), and RCP85 and SSP5-85 (f). The blue solid line shows the "prior" CDF for CMIP5 and CMIP6. The other solid lines represent CDF constrained with background nitrate in WOA18 (orange) and GLODAPv2 (red). All three distributions represented by solid lines are assumed to be a Gaussian distribution. The hatched histogram represents CDF for the chlorophyll changes directly calculated among 26 CMIP5 and CMIP6 ESMs. Scatters illustrate the cumulative probability where future chlorophyll changes are projected to decrease. Mean and standard deviation of chlorophyll changes without and with EC are provided in Table 1. Out-of-sample testing is applied across different ESM ensembles.

and CMIP6 ESMs (Figure S10a in Supporting Information S1). Similarly, changes in Arctic marine productivity can be estimated by applying the emergent constraint to the background nitrate concentration.

4. Conclusion and Discussion

In recent decades, the Arctic Ocean has experienced major changes in environmental conditions such as increased surface temperatures, reduced sea ice extent, and intensified stratification. These physical changes have affected ocean productivity and the phytoplankton biomass (Ardyna & Arrigo, 2020). We investigated the projected changes in the chlorophyll concentration in the Arctic Ocean. The present result exhibits that the large spread of inter-model diversity exists among the projections based on CMIP5 and CMIP6 ESMs, which is consistent with the high degree of uncertainty in the projections of Arctic phytoplankton biomass in CMIP5 (Cabré et al., 2014) and CMIP6 (Kwiatkowski et al., 2020). The range of values for the background nitrate concentration used in the CMIP5 models was large (Vancoppenolle et al., 2013), and this range has become even wider in the CMIP6 models. The remarkably strong correlation (0.86, $P < 0.001$) between the background nitrate concentration and the change in the chlorophyll concentration suggests that the background nitrate concentration is key to determining future chlorophyll levels in the Arctic Ocean. Constraining the observed nitrate to the linear relationship between the background nitrate concentration and the chlorophyll projections, the chlorophyll concentration is estimated to decrease by 45%–51% relative to current levels, which is about three-fold than the reduction projected by the multi-model mean (14%). Based on the estimation using emergent constraint, the uncertainty in the direction of chlorophyll changes is reduced and we can assure the future chlorophyll decline with over 90% probability.

Although the biogeochemical fields in the ESMs are all initialized using similar observational datasets that are based on WOA and GLODAP data (Séférian, Delire, et al., 2016), the simulations of the nitrate concentration in the Arctic Ocean produce a large inter-model spread. In addition, some of the newly developed ESMs have a serious systematic bias in the nutrient distribution. The amount of nitrate in the Arctic Ocean is controlled by both physical and biological processes. Physical processes that can affect the nutrient concentrations include winter vertical mixing (Randelhoff et al., 2020; Wiedmann et al., 2017), which supplies nutrient-rich deep water to the ocean surface; and horizontal transport from the Pacific and Atlantic sectors (Henley et al., 2020; Randelhoff et al., 2018), which contain higher concentrations of nitrate than the central Arctic basin; riverine nutrient inputs (Carmack et al., 2016; Terhaar et al., 2019); coastal erosion (Fritz et al., 2017; Terhaar, Lauerwald, et al., 2021); and atmospheric nitrogen deposition (Krishnamurthy et al., 2009; Somes et al., 2016). Additionally, nitrate concentrations are controlled by biological sources and sinks, such as nitrogen fixation and assimilation, denitrification, and anammox by microorganisms (Wang et al., 2019; Wrightson & Tagliabue, 2020; Zakem et al., 2018). In the nitrogen cycle, the interactions between the above physical and biological properties are not fully accounted for in the current generation of ESMs. In particular, large amounts of nutrient recycling by microorganisms and overestimated nutrient fluxes may be the reason for the overestimated nitrate concentrations in CMIP6 (Wang et al., 2019).

The increase in Arctic NPP has been observed over the last 20 years (Arrigo & van Dijken, 2011, 2015; Lewis et al., 2020) and the positive trend in chlorophyll concentration are recently reported (Lewis et al., 2020), which is opposite to the CMIP5 and CMIP6 chlorophyll projections. The observed positive trend is mainly due to increase in the summer chlorophyll, while the majority of CMIP5 and CMIP6 models simulate a significant negative trend in the summer chlorophyll until the end of the 21st century. This increase in productivity has been attributed to the increased light availability due to the retreat of the sea-ice extent (Arrigo & van Dijken, 2015) as sea-ice was covered in the substantial Arctic Ocean even during the boreal summer. As the sea-ice extent is rapidly reduced, the chlorophyll increase due to increased light availability will be limited to a narrow area around the permanent sea-ice in the boreal summer. Instead, the time at which the effect of the light availability will be seasonally earlier than present climate, eventually in boreal spring, which is consistent with the model projection. The current positive chlorophyll trends, sustained by the nutrient supplies (Lewis et al., 2020) might not be persisted as the nutrient limitation gets severe in the response to the global warming, implying that the Arctic phytoplankton dynamics may slowly change from the light limitation to the nutrient limitation. This shift will play an important role chlorophyll changes in the Arctic.

Data Availability Statement

The nitrate in WOA18 and GLODAPv2 are provided freely at https://www.ncei.noaa.gov/access/world-ocean-atlas-2018/bin/woa18oxnu.pl?parameter=n and https://www.ncei.noaa.gov/data/oceans/ncei/ocads/data/0162565/, respectively. The CMIP5 and CMIP6 archives are freely available from https://esgf-node.llnl.gov/. All figures

were generated by using software package Python with the matplotlib and basemap modules (https://matplotlib.org/, https://matplotlib.org/basemap/). The map coastlines are derived by the Global Self-consistent, Hierarchical, High-resolution Geography (GSHHG) Database (www.soest.hawaii.edu/pwessel/gshhg/), which has been distributed under the GNU Lesser General Public License and is provided with the basemap Python module.

Acknowledgments
The authors thank fruitful discussions about Arctic climate and chlorophyll responses with John P. Dunne (NOAA-GFDL) and Charles A Stock (NOAA-GFDL). The authors also appreciate valuable comments for elevating the quality of the manuscript from two anonymous reviewers. This research was supported by KIMST funded by the Ministry of Oceans and Fisheries (20210605, Korea-Arctic Ocean Warming and Response of Ecosystem, KOPRI), and supported by the National Research Foundation of Korea (NRF-2022R1A3B1077622). This report was also prepared by H.-G. Lim under award NA18OAR4320123 from the National Oceanic and Atmospheric Administration, U.S. Department of Commerce. The statements, findings, conclusions, and recommendations are those of the author(s) and do not necessarily reflect the views of the National Oceanic and Atmospheric Administration, or the U.S. Department of Commerce.

References

Ahmed, R., Prowse, T., Dibike, Y., Bonsal, B., & O'Neil, H. (2020). Recent trends in freshwater influx to the Arctic Ocean from four major arctic-draining rivers. *Water*, *12*(4), 1189. https://doi.org/10.3390/w12041189

AMAP. (2017). *Snow, water, ice and permafrost in the Arctic (SWIPA)*. AMAP.

Ardyna, M., & Arrigo, K. R. (2020). Phytoplankton dynamics in a changing Arctic Ocean. *Nature Climate Change*, *10*(10), 1–12. https://doi.org/10.1038/s41558-020-0905-y

Arrigo, K. R., & van Dijken, G. L. (2011). Secular trends in Arctic Ocean net primary production. *Journal of Geophysical Research*, *116*(C9), C09011. https://doi.org/10.1029/2011jc007151

Arrigo, K. R., & van Dijken, G. L. (2015). Continued increases in Arctic Ocean primary production. *Progress in Oceanography*, *136*, 60–70. https://doi.org/10.1016/j.pocean.2015.05.002

Assmy, P., Fernández-Méndez, M., Duarte, P., Meyer, A., Randelhoff, A., Mundy, C. J., et al. (2017). Leads in Arctic pack ice enable early phytoplankton blooms below snow-covered sea ice. *Scientific Reports*, *7*, 1–9. https://doi.org/10.1038/srep40850

Behrenfeld, M. J., Boss, E., Siegel, D. A., & Shea, D. M. (2005). Carbon-based ocean productivity and phytoplankton physiology from space. *Global Biogeochemical Cycles*, *19*(1), 57–14. https://doi.org/10.1029/2004gb002299

Behrenfeld, M. J., & Falkowski, P. G. (1997). Photosynthetic rates derived from satellite-based chlorophyll concentration. *Limnology & Oceanography*, *42*, 1–20. https://doi.org/10.4319/lo.1997.42.1.0001

Boe, J. L., Hall, A., & Qu, X. (2009). September sea-ice cover in the Arctic Ocean projected to vanish by 2100. *Nature Geoscience*, *2*(5), 341–343. https://doi.org/10.1038/ngeo467

Bopp, L., Resplandy, L., Orr, J. C., Doney, S. C., Dunne, J. P., Gehlen, M., et al. (2013). Multiple stressors of ocean ecosystems in the 21st century: Projections with CMIP5 models. *Biogeosciences*, *10*, 6225–6245. https://doi.org/10.5194/bg-10-6225-2013

Bracegirdle, T. J., & Stephenson, D. B. (2013). On the robustness of emergent constraints used in multimodel climate change projections of Arctic warming. *Journal of Climate*, *26*(2), 669–678. https://doi.org/10.1175/jcli-d-12-00537.1

Brient, F., Schneider, T., Tan, Z., Bony, S., Qu, X., & Hall, A. (2016). Shallowness of tropical low clouds as a predictor of climate models' response to warming. *Climate Dynamics*, *47*(1–2), 433–449. https://doi.org/10.1007/s00382-015-2846-0

Cabré, A., Marinov, I., & Leung, S. (2014). Consistent global responses of marine ecosystems to future climate change across the IPCC AR5 Earth system models. *Climate Dynamics*, *45*(5–6), 1253–1280. https://doi.org/10.1007/s00382-014-2374-3

Carmack, E. C., Yamamoto Kawai, M., Haine, T. W. N., Bacon, S., Bluhm, B. A., Lique, C., et al. (2016). Freshwater and its role in the Arctic Marine System: Sources, disposition, storage, export, and physical and biogeochemical consequences in the Arctic and global oceans. *Journal of Geophysical Research: Biogeosciences*, *121*(3), 675–717. https://doi.org/10.1002/2015jg003140

Cox, P. M., Pearson, D., Booth, B. B., Friedlingstein, P., Huntingford, C., Jones, C. D., & Luke, C. M. (2013). Sensitivity of tropical carbon to climate change constrained by carbon dioxide variability. *Nature*, *494*(7437), 341–344. https://doi.org/10.1038/nature11882

Davy, R., & Outten, S. (2021). The arctic surface climate in CMIP6: Status and developments since CMIP5. *Journal of Climate*, *33*(18), 8047–8068. https://doi.org/10.1175/jcli-d-19-0990.1

Eyring, V., Bony, S., Meehl, G. A., Senior, C. A., Stevens, B., Stouffer, R. J., & Taylor, K. E. (2016). Overview of the coupled model intercomparison project phase 6 (CMIP6) experimental design and organization. *Geoscientific Model Development*, *9*(5), 1937–1958. https://doi.org/10.5194/gmd-9-1937-2016

Fritz, M., Vonk, J. E., & Lantuit, H. (2017). Collapsing arctic coastlines. *Nature Climate Change*, *7*(1), 6–7. https://doi.org/10.1038/nclimate3188

Fujiwara, A., Hirawake, T., Suzuki, K., Eisner, L., Imai, I., Nishino, S., et al. (2016). Influence of timing of sea ice retreat on phytoplankton size during marginal ice zone bloom period on the Chukchi and Bering shelves. *Biogeosciences*, *13*(1), 115–131. https://doi.org/10.5194/bg-13-115-2016

Garcia, H. E., Weathers, K. W., Paver, C. R., Smolyar, I., Boyer, T. P., Locarnini, R. A., et al. (2018). In A. Mishonov (Ed.), (Technical editor), *World Ocean Atlas 2018. Vol. 4: Dissolved inorganic nutrients (phosphate, nitrate and nitrate+nitrite, silicate). NOAA Atlas NESDIS* (Vol. 84, 35 pp.).

Hall, A., Cox, P., Huntingford, C., & Klein, S. (2019). Progressing emergent constraints on future climate change. *Nature Climate Change*, *9*(4), 1–10. https://doi.org/10.1038/s41558-019-0436-6

Hartmann, D. L., Klein Tank, A. M. G., Rusticucci, M., Alexander, L. V., Brönnimann, S., Charabi, Y., et al. (2013). Observations: Atmosphere and surface. In Intergovernmental Panel on Climate Change (ed.), *Climate change 2013 – The physical science basis: Working group I contribution to the fifth assessment report of the Intergovernmental Panel on Climate Change* (pp. 159–254). Cambridge University Press.

Henley, S. F., Porter, M., Hobbs, L., Braun, J., Guillaume-Castel, R., Venables, E. J., et al. (2020). Nitrate supply and uptake in the Atlantic Arctic sea ice zone: Seasonal cycle, mechanisms and drivers. *Philosophical Transactions of the Royal Society A: Mathematical, Physical & Engineering Sciences*, *378*(2181), 20190361. https://doi.org/10.1098/rsta.2019.0361

Jönsson, B. F., Sathyendranath, S., & Platt, T. (2020). Trends in winter light environment over the Arctic Ocean: A perspective from two decades of ocean color data. *Geophysical Research Letters*, *47*(16), 1–9. https://doi.org/10.1029/2020gl089037

Kahru, M., Brotas, V., Manzano-Sarabia, M., & Mitchell, B. G. (2011). Are phytoplankton blooms occurring earlier in the Arctic? *Global Change Biology*, *17*(4), 1733–1739. https://doi.org/10.1111/j.1365-2486.2010.02312.x

Krishnamurthy, A., Moore, J. K., Mahowald, N., Luo, C., Doney, S. C., Lindsay, K., & Zender, C. S. (2009). Impacts of increasing anthropogenic soluble iron and nitrogen deposition on ocean biogeochemistry. *Global Biogeochemical Cycles*, *23*(3), 1–15. https://doi.org/10.1029/2008gb003440

Kwiatkowski, L., Bopp, L., Aumont, O., Ciais, P., Cox, P. M., Laufkötter, C., et al. (2017). Emergent constraints on projections of declining primary production in the tropical oceans. *Nature Climate Change*, *7*(5), 355–358. https://doi.org/10.1038/nclimate3265

Kwiatkowski, L., Torres, O., Bopp, L., Aumont, O., Chamberlain, M., Christian, J. R., et al. (2020). Twenty-first century ocean warming, acidification, deoxygenation, and upper-ocean nutrient and primary production decline from CMIP6 model projections. *Biogeosciences*, *17*(13), 3439–3470. https://doi.org/10.5194/bg-17-3439-2020

Kwok, R. (2018). Arctic sea ice thickness, volume, and multiyear ice coverage: Losses and coupled variability (1958–2018). *Environmental Research Letters*, *13*(10), 105005. https://doi.org/10.1088/1748-9326/aae3ec

Lammers, R. B., Shiklomanov, A. I., Vörösmarty, C. J., Fekete, B. M., & Peterson, B. J. (2001). Assessment of contemporary Arctic river runoff based on observational discharge records. *Journal of Geophysical Research*, *106*(D4), 3321–3334. https://doi.org/10.1029/2000jd900444

Laufkotter, C., Vogt, M., Gruber, N., Aita-Noguchi, M., Aumont, O., Bopp, L., et al. (2015). Drivers and uncertainties of future global marine primary production in marine ecosystem models. *Biogeosciences*, *12*(23), 6955–6984. https://doi.org/10.5194/bg-12-6955-2015

Lauvset, S. K., Key, R. M., Olsen, A., van Heuven, S., Velo, A., Lin, X., et al. (2016). A new global interior ocean mapped climatology: The 1° × 1° GLODAP version 2. *Earth System Science Data*, *8*, 325–340. https://doi.org/10.5194/essd-8-325-2016

Lee, Y., Min, J.-O., Yang, E. J., Cho, K.-H., Jung, J., Park, J., et al. (2019). Influence of sea ice concentration on phytoplankton community structure in the Chukchi and East Siberian Seas, Pacific Arctic Ocean. *Deep-Sea Research Part I*, *147*, 54–64. https://doi.org/10.1016/j.dsr.2019.04.001

Lengaigne, M., Madec, G., Bopp, L., Menkes, C., Aumont, O., & Cadule, P. (2009). Bio-physical feedbacks in the Arctic Ocean using an Earth system model. *Geophysical Research Letters*, *36*(21), 401–405. https://doi.org/10.1029/2009gl040145

Lewis, K. M., van Dijken, G. L., & Arrigo, K. R. (2020). Changes in phytoplankton concentration now drive increased Arctic Ocean primary production. *Science*, *369*(6500), 198–202. https://doi.org/10.1126/science.aay8380

Li, G., Xie, S.-P., He, C., & Chen, Z. (2017). Western Pacific emergent constraint lowers projected increase in Indian summer monsoon rainfall. *Nature Climate Change*, *7*(10), 708–712. https://doi.org/10.1038/nclimate3387

Lim, H.-G., Kug, J.-S., & Park, J.-Y. (2019a). Biogeophysical feedback of phytoplankton on the Arctic climate. Part I: Impact of nonlinear rectification of interactive chlorophyll variability in the present-day climate. *Climate Dynamics*, *52*(9–10), 5383–5396. https://doi.org/10.1007/s00382-018-4450-6

Lim, H.-G., Kug, J.-S., & Park, J.-Y. (2019b). Biogeophysical feedback of phytoplankton on Arctic climate. Part II: Arctic warming amplified by interactive chlorophyll under greenhouse warming. *Climate Dynamics*, *53*(5–6), 3167–3180. https://doi.org/10.1007/s00382-019-04693-5

Long, M. C., Moore, J. K., Lindsay, K., Lévy, M., Doney, S. C., Luo, Y. J., et al. (2021). Simulations with the Marine Biogeochemistry Library (MARBL). *Journal of Advances in Modeling Earth Systems*, *13*(12), e2021MS002647. https://doi.org/10.1029/2021ms002647

Manizza, M., Le Quéré, C., Watson, A. J., & Buitenhuis, E. T. (2005). Bio-optical feedbacks among phytoplankton, upper ocean physics and sea-ice in a global model. *Geophysical Research Letters*, *32*(5), L05603. https://doi.org/10.1029/2004GL020778

Michaelis, L., & Menten, M. (1913). Die Kinetik der Invertiiiwirkulig. *Biochemische*, 333–369.

Moss, R. H., Edmonds, J. A., Hibbard, K. A., Manning, M. R., Rose, S. K., van Vuuren, D. P., et al. (2010). The next generation of scenarios for climate change research and assessment. *Nature*, *463*(7282), 1–10. https://doi.org/10.1038/nature08823

Neeley, A. R., Harris, L. A., & Frey, K. E. (2018). Unraveling phytoplankton community dynamics in the Northern Chukchi sea under sea-ice-covered and sea-ice-free conditions. *Geophysical Research Letters*, *45*(15), 7663–7671. https://doi.org/10.1029/2018gl077684

Notz, D., & SIMIP Community. (2020). Arctic Sea ice in CMIP6. *Geophysical Research Letters*, *47*(10), 1–11. https://doi.org/10.1029/2019gl086749

O'Gorman, P. A. (2012). Sensitivity of tropical precipitation extremes to climate change. *Nature Geoscience*, *5*(10), 697–700. https://doi.org/10.1038/ngeo1568

O'Neill, B. C., Tebaldi, C., van Vuuren, D. P., Eyring, V., Friedlingstein, P., Hurtt, G., et al. (2016). The Scenario Model Intercomparison Project (ScenarioMIP) for CMIP6. *Geoscientific Model Development*, *9*, 3461–3482. https://doi.org/10.5194/gmd-9-3461-2016

Park, J.-Y., Kug, J.-S., Bader, J., Rolph, R., & Kwon, M. (2015). Amplified Arctic warming by phytoplankton under greenhouse warming. *Proceedings of the National Academy of Sciences of the United States of America*, *112*(19), 5921–5926. https://doi.org/10.1073/pnas.1416884112

Peterson, B. J., Holmes, R. M., McClelland, J. W., Vörösmarty, C. J., Lammers, R. B., Shiklomanov, A. I., et al. (2002). Increasing river discharge to the Arctic Ocean. *Science*, *298*(5601), 2171–2173. https://doi.org/10.1126/science.1077445

Polyakov, I. V., Pnyushkov, A. V., & Carmack, E. C. (2018). Stability of the arctic halocline: A new indicator of arctic climate change. *Environmental Research Letters*, *13*(12). https://doi.org/10.1088/1748-9326/aaec1e

Polyakov, I. V., Rippeth, T. P., Fer, I., Baumann, T. M., Carmack, E. C., Ivanov, V. V., et al. (2020). Intensification of near-surface currents and shear in the Eastern Arctic Ocean. *Geophysical Research Letters*, *47*(16), 11–19. https://doi.org/10.1029/2020gl089469

Randelhoff, A., Holding, J., Janout, M., Sejr, M. K., Babin, M., Tremblay, J.-E., & Alkire, M. B. (2020). Pan-Arctic ocean primary production constrained by turbulent nitrate fluxes. *Frontiers in Marine Science*, *7*, 1–15. https://doi.org/10.3389/fmars.2020.00150

Randelhoff, A., Reigstad, M., Chierici, M., Sundfjord, A., Ivanov, V., Cape, M., et al. (2018). Seasonality of the physical and biogeochemical hydrography in the inflow to the Arctic Ocean through Fram Strait. *Frontiers in Marine Science*, *5*, 224. https://doi.org/10.3389/fmars.2018.00224

Sarthou, G., Timmermans, K. R., Blain, S., & Treguer, P. (2005). Growth physiology and fate of diatoms in the ocean: A review. *Journal of Sea Research*, *53*(1–2), 25–42. https://doi.org/10.1016/j.seares.2004.01.007

Schulzweida, U. (2019). CDO user guide (pp. 1–230).

Séférian, R., Berthet, S., Yool, A., Palmieri, J., Bopp, L., Tagliabue, A., et al. (2020). Tracking improvement in simulated marine biogeochemistry between CMIP5 and CMIP6. *Current Climate Change Reports*, *6*(3), 95–119. https://doi.org/10.1007/s40641-020-00160-0

Séférian, R., Gehlen, M., Bopp, L., Resplandy, L., Orr, J. C., Marti, O., et al. (2016). Inconsistent strategies to spin up models in CMIP5: Implications for ocean biogeochemical model performance assessment. *Geoscientific Model Development*, *9*(5), 1827–1851. https://doi.org/10.5194/gmd-9-1827-2016

Simpson, K. G., Tremblay, J.-É., Gratton, Y., & Price, N. M. (2008). An annual study of inorganic and organic nitrogen and phosphorus and silicic acid in the southeastern Beaufort Sea. *Journal of Geophysical Research*, *113*(C7), 65–16. https://doi.org/10.1029/2007jc004462

Somes, C. J., Landolfi, A., Koeve, W., & Oschlies, A. (2016). Limited impact of atmospheric nitrogen deposition on marine productivity due to biogeochemical feedbacks in a global ocean model. *Geophysical Research Letters*, *43*(9), 4500–4509. https://doi.org/10.1002/2016gl068335

Stock, C. A., Dunne, J. P., Fan, S., Ginoux, P., John, J., Krasting, J. P., et al. (2020). Ocean biogeochemistry in GFDL's Earth system Model 4.1 and its response to increasing atmospheric CO_2. *Journal of Advances in Modeling Earth Systems*, *12*(10), e2019MS002043. https://doi.org/10.1029/2019ms002043

Tagliabue, A., Kwiatkowski, L., Bopp, L., Butenschon, M., Cheung, W., Lengaigne, M., & Vialard, J. (2021). Persistent uncertainties in ocean net primary production climate change projections at regional scales raise challenges for assessing impacts on ecosystem services. *Frontiers in Climate*, *3*, 149–166. https://doi.org/10.3389/fclim.2021.738224

Taylor, K. E., Stouffer, R. J., & Meehl, G. A. (2012). An overview of CMIP5 and the experiment design. *Bulletin of the American Meteorological Society*, *93*(4), 485–498. https://doi.org/10.1175/bams-d-11-00094.1

Terhaar, J., Frölicher, T. L., & Joos, F. (2021). Southern Ocean anthropogenic carbon sink constrained by sea surface salinity. *Science Advances*, *7*(18), 5964–5992. https://doi.org/10.1126/sciadv.abd5964

Terhaar, J., Kwiatkowski, L., & Bopp, L. (2020). Emergent constraint on Arctic Ocean acidification in the twenty-first century. *Nature*, *582*(7812), 379–383. https://doi.org/10.1038/s41586-020-2360-3

Terhaar, J., Lauerwald, R., Regnier, P., Gruber, N., & Bopp, L. (2021). Around one third of current Arctic Ocean primary production sustained by rivers and coastal erosion. *Nature Communications*, *12*, 1–10. https://doi.org/10.1038/s41467-020-20470-z

Terhaar, J., Orr, J. C., Ethé, C., Regnier, P., & Bopp, L. (2019). Simulated Arctic Ocean response to doubling of riverine carbon and nutrient delivery. *Global Biogeochemical Cycles*, *33*(8), 1048–1070. https://doi.org/10.1029/2019gb006200

Timmermans, M. L., & Marshall, J. (2020). Understanding Arctic Ocean circulation: A review of ocean dynamics in a changing climate. *Journal of Geophysical Research: Oceans*, *125*(4), C04S02–35. https://doi.org/10.1029/2018jc014378

Toole, J. M., Timmermans, M. L., Perovich, D. K., Krishfield, R. A., Proshutinsky, A., & Richter-Menge, J. A. (2010). Influences of the ocean surface mixed layer and thermohaline stratification on Arctic Sea ice in the central Canada Basin. *Journal of Geophysical Research*, *115*, C10018. https://doi.org/10.1029/2009jc005660

Tremblay, J.-E., Anderson, L. G., Matrai, P., Coupel, P., Bélanger, S., Michel, C., & Reigstad, M. (2015). Global and regional drivers of nutrient supply, primary production and CO_2 drawdown in the changing Arctic Ocean. *Progress in Oceanography*, *139*, 171–196. https://doi.org/10.1016/j.pocean.2015.08.009

Tremblay, J.-É., & Gagnon, J. (2009). The effects of irradiance and nutrient supply on the productivity of arctic waters: A perspective on climate change. In J. C. J. Nihoul, & A. G. Kostianoy (Eds.), *Influence of climate change on the changing Arctic and Sub-Arctic conditions* (pp. 73–93). Springer.

Tremblay, J.-É., Michel, C., Hobson, K. A., Gosselin, M., & Price, N. M. (2006). Bloom dynamics in early opening waters of the Arctic Ocean. *Limnology & Oceanography*, *51*(2), 900–912. https://doi.org/10.4319/lo.2006.51.2.0900

Vancoppenolle, M., Bopp, L., Madec, G., Dunne, J., Ilyina, T., Halloran, P. R., & Steiner, N. (2013). Future Arctic Ocean primary productivity from CMIP5 simulations: Uncertain outcome, but consistent mechanisms. *Global Biogeochemical Cycles*, *27*(3), 605–619. https://doi.org/10.1002/gbc.20055

Wang, W.-L., Moore, J. K., Martiny, A. C., & Primeau, F. W. (2019). Convergent estimates of marine nitrogen fixation. *Nature*, *566*(7743), 1–9. https://doi.org/10.1038/s41586-019-0911-2

Wassmann, P., & Reigstad, M. (2011). Future Arctic Ocean seasonal ice zones and implications for pelagic-benthic coupling. *Oceanography*, *24*(3), 220–231. https://doi.org/10.5670/oceanog.2011.74

Wiedmann, I., Tremblay, J.-É., & Reigstad, A. S. A. M. (2017). Upward nitrate flux and downward particulate organic carbon flux under contrasting situations of stratification and turbulent mixing in an Arctic shelf sea. *Elem Sci Anth*, *43*, 1–15.

Wrightson, L., & Tagliabue, A. (2020). Quantifying the impact of climate change on marine diazotrophy: Insights from Earth system models. *Frontiers in Marine Science*, *7*, 1–9. https://doi.org/10.3389/fmars.2020.00635

Yamaguchi, R., Rodgers, K. B., Timmermann, A., Stein, K., Schlunegger, S., Bianchi, D., et al. (2022). Trophic level decoupling drives future changes in phytoplankton bloom phenology. *Nature Climate Change*, *12*(5), 469–476. https://doi.org/10.1038/s41558-022-01353-1

Yamamoto-Kawai, M., Carmack, E., & McLaughlin, F. (2006). Nitrogen balance and Arctic throughflow. *Nature*, *443*(7107), 43–3. https://doi.org/10.1038/443043a

Zakem, E. J., Al-Haj, A., Church, M. J., Dijken, G. L., Dutkiewicz, S., Foster, S. Q., et al. (2018). Ecological control of nitrite in the upper ocean. *Nature Communications*, *9*, 1–13. https://doi.org/10.1038/s41467-018-03553-w

Zelinka, M. D., Myers, T. A., McCoy, D. T., Po Chedley, S., Caldwell, P. M., Ceppi, P., et al. (2020). Causes of higher climate sensitivity in CMIP6 models. *Geophysical Research Letters*, *47*, e2019GL085782. https://doi.org/10.1029/2019gl085782

Zhai, C., Jiang, J. H., & Su, H. (2015). Long-term cloud change imprinted in seasonal cloud variation: More evidence of high climate sensitivity. *Geophysical Research Letters*, *42*(20), 8729–8737. https://doi.org/10.1002/2015gl065911

References From the Supporting Information

Arora, V. K., Scinocca, J. F., Boer, G. J., Christian, J. R., Denman, K. L., Flato, G. M., et al. (2011). Carbon emission limits required to satisfy future representative concentration pathways of greenhouse gases. *Geophysical Research Letters*, *38*(5). https://doi.org/10.1029/2010gl046270

Boucher, O., Servonnat, J., Albright, A. L., Aumont, O., Balkanski, Y., Bastrikov, V., et al. (2020). Presentation and evaluation of the IPSL-CM6A-LR climate model. *Journal of Advances in Modeling Earth Systems*, *12*(7), 1029–1052. https://doi.org/10.1029/2019ms002010

Danabasoglu, G., Lamarque, J. F., Bacmeister, J., Bailey, D. A., DuVivier, A. K., Edwards, J., et al. (2020). The Community Earth System Model Version 2 (CESM2). *Journal of Advances in Modeling Earth Systems*, *12*, 106–135. https://doi.org/10.1029/2019ms001916

Dufresne, J. L., Foujols, M. A., Denvil, S., Caubel, A., Marti, O., Aumont, O., et al. (2013). Climate change projections using the IPSL-CM5 Earth system model: From CMIP3 to CMIP5. *Climate Dynamics*, *40*(9–10), 2123–2165. https://doi.org/10.1007/s00382-012-1636-1

Dunne, J. P., Horowitz, L. W., Adcroft, A. J., Ginoux, P., Held, I. M., John, J. G., et al. (2020). The GFDL Earth System Model Version 4.1 (GFDL-ESM 4.1): Overall coupled model description and simulation characteristics. *Journal of Advances in Modeling Earth Systems*, *12*(11), e2019MS002015. https://doi.org/10.1029/2019ms002015

Dunne, J. P., John, J. G., Adcroft, A. J., Griffies, S. M., Hallberg, R. W., Shevliakova, E., et al. (2012). GFDL's ESM2 global coupled climate–carbon Earth system models. Part I: Physical formulation and baseline simulation characteristics. *Journal of Climate*, *25*(19), 6646–6665. https://doi.org/10.1175/jcli-d-11-00560.1

Giorgetta, M. A., Jungclaus, J., Reick, C. H., Legutke, S., Bader, J., Böttinger, M., et al. (2013). Climate and carbon cycle changes from 1850 to 2100 in MPI-ESM simulations for the Coupled Model Intercomparison Project phase 5. *Journal of Advances in Modeling Earth Systems*, *5*(3), 572–597. https://doi.org/10.1002/jame.20038

Hajima, T., Watanabe, M., Yamamoto, A., Tatebe, H., Noguchi, M. A., Abe, M., et al. (2020). Development of the MIROC-ES2L Earth system model and the evaluation of biogeochemical processes and feedbacks. *Geoscientific Model Development*, *13*(5), 2197–2244. https://doi.org/10.5194/gmd-13-2197-2020

Jones, C. D., Hughes, J. K., Bellouin, N., Hardiman, S. C., Jones, G. S., Knight, J., et al. (2011). The HadGEM2-ES implementation of CMIP5 centennial simulations. *Geoscientific Model Development*, *4*(3), 543–570. https://doi.org/10.5194/gmd-4-543-2011

Lindsay, K., Bonan, G. B., Doney, S. C., Hoffman, F. M., Lawrence, D. M., Long, M. C., et al. (2014). Preindustrial-control and twentieth-century carbon cycle experiments with the Earth system model CESM1(BGC). *Journal of Climate*, *27*(24), 8981–9005. https://doi.org/10.1175/jcli-d-12-00565.1

Mauritsen, T., Bader, J., Becker, T., Behrens, J., Bittner, M., Brokopf, R., et al. (2019). Developments in the MPI-M Earth system model version 1.2 (MPI-ESM1.2) and its response to increasing CO_2. *Journal of Advances in Modeling Earth Systems*, *11*(4), 998–1038. https://doi.org/10.1029/2018ms001400

Romanou, A., Gregg, W. W., Romanski, J., Kelley, M., Bleck, R., Healy, R., et al. (2013). Natural air-sea flux of CO_2 in simulations of the NASA-GISS climate model: Sensitivity to the physical ocean model formulation. *Ocean Modelling*, *66*, 26–44. https://doi.org/10.1016/j.ocemod.2013.01.008

Seland, Ø., Bentsen, M., Olivié, D., Toniazzo, T., Gjermundsen, A., Graff, L. S., et al. (2020). Overview of the Norwegian Earth System Model (NorESM2) and key climate response of CMIP6 DECK, historical, and scenario simulations. *Geoscientific Model Development*, *13*(12), 6165–6200. https://doi.org/10.5194/gmd-13-6165-2020

Sellar, A. A., Jones, C. G., Mulcahy, J. P., Tang, Y., Yool, A., Wiltshire, A., et al. (2019). UKESM1: Description and evaluation of the UK Earth system model. *Journal of Advances in Modeling Earth Systems*, *11*(12), 4513–4558. https://doi.org/10.1029/2019ms001739

Séférian, R., Delire, C., Decharme, B., Voldoire, A., Salas y Mélia, D., Chevallier, M., et al. (2016). Development and evaluation of CNRM Earth system model - CNRM-ESM1. *Geoscientific Model Development*, *9*(4), 1423–1453. https://doi.org/10.5194/gmd-9-1423-2016

Séférian, R., Nabat, P., Michou, M., Saint-Martin, D., Voldoire, A., Colin, J., et al. (2019). Evaluation of CNRM Earth system model, CNRM-ESM2-1: Role of Earth system processes in present-day and future climate. *Journal of Advances in Modeling Earth Systems*, *11*(12), 4182–4227. https://doi.org/10.1029/2019ms001791

Swart, N. C., Cole, J. N. S., Kharin, V. V., Lazare, M., Scinocca, J. F., Gillett, N. P., et al. (2019). The Canadian Earth system model version 5 (CanESM5.0.3). *Geoscientific Model Development*, *12*(11), 4823–4873. https://doi.org/10.5194/gmd-12-4823-2019

Ziehn, T., Chamberlain, M. A., Law, R. M., Lenton, A., Bodman, R. W., Dix, M., et al. (2020). The Australian Earth system model: ACCESS-ESM1.5. *Journal of Southern Hemisphere Earth Systems Science*, *70*(1), 193–214. https://doi.org/10.1071/es19035